Inorganic Chemistry

Article

pubs.acs.org/IC

Syntheses and Characterization of Salts with the $[Al(D)_4F_2]^+$ Cation (D = Pyridine or Water)

Anton Dimitrov,[†] Detlef Heidemann,[†] Khalaf I. Khallow,[‡] and Erhard Kemnitz*,[†]

[†]Institute of Chemistry, Humboldt University of Berlin, Brook-Taylor-Str. 2, 12489 Berlin, Germany

[‡]Department of Chemistry, College of Education, University of Mosul, Iraq

Supporting Information

ABSTRACT: Our approach for preparation of *tetrakis*-(pyridine)-difluoro-aluminum chloride was successfully deployed for the synthesis of corresponding Br and I compounds, respectively. By reacting $AlX_3 \cdot 3Py$ (X = Cl, Br, I) with Me_3SiF in pyridine, two of the three halogens X were substituted by fluorine atoms forming the "aluminum mixed halide" complexes $AlF_2X \cdot 4Py$ with the ionic solid-state structures $[Al(Py)_4F_2]X$. Whereas the ^{27}Al solid state NMR spectra of $AlX_3 \cdot 3Py$ (X = Cl, Br) confirmed the existence of the expected singular $\sigma^6\lambda^3$-Al centers in their structures, the corresponding spectrum of $AlI_3 \cdot 3Py$ does not contain any signal that belongs to a 6-fold coordinated Al atom. The elemental analysis data strongly support the 1:2-stoichiometry of the complex ($AlI_3 \cdot 2Py$), which in accord to the ^{27}Al MAS NMR spectra possessed only one $\sigma^4\lambda^3$-Al side as in the ionic structure $[Al(Py)_2I_2]I$. $AlBr_3 \cdot 3Py$ was also transformed by pyridine into the ionic complex $[Al(Py)_4Br_2]Br$. The later was isolated from pyridine solutions, and its structure was determined by X-ray single crystal analysis. On the basis of our results, solvated $[Al(Py)_nX_2]^+$ cations are most probably the dominating species in pyridine solutions of AlX_3. Thus, only two Al−X covalent bonds underwent X/F- exchange and the halogen exchange reactions were terminated at " $[Al(Py)_4F_2]^+$ stage". The hydrolysis of $[Al(Py)_4F_2]Cl$ by very diluted hydrochloric acid in methanol proceeded smoothly under preservation of the Al−F bonds and displacement of pyridine by water. The formation of the stable helical *trans*-octahedron $[Al(H_2O)_4F_2]^+$ cation was confirmed by single-crystal XRD analysis. By reacting $[Al(Py)_4F_2]Cl$ with the *cyclo-n*-propyl-phosphonic acid anhydride $[CH_3CH_2CH_2{-}PO_2]_3$, an unexpected F-migration from Al- to P- atoms was observed.

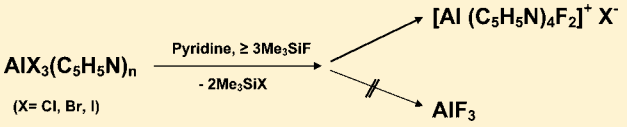

1. INTRODUCTION

Though highly exothermic, the halogen-exchange reactions of solid $AlCl_3$ or $AlBr_3$ with liquid CCl_3F can easily be controlled and directed to catalytically interesting amorphous "AlF_3 phases". The halogen exchange can not be performed to completeness and the remaining traces of the heavy halogens (Cl, Br) are inducing somehow the "chemical distorted" AlF_3 phases: ACF ($AlCl_xF_{3-x}$, x = 0.05 ... 0.30) and ABF ($AlBr_xF_{3-x}$, x = 0.05 ... 0.30).[1−4] Both compounds belong to the strongest Lewis acids, and to the very limited number of solid acids among them, which are able to catalyze the same reactions as efficiently as liquid SbF_5.[5] No uniform product could be obtained by performing the analogous reaction between CCl_3F and AlI_3.[6] As previously demonstrated, the halogen exchange reaction with CCl_3F can dramatically be influenced and completely stopped if $AlCl_3 \cdot 3Py$ (**1a**) is used as reactant instead of $AlCl_3$.[7] However, the desired halogen exchange at **1a** occurs easily with Me_3SiF in pyridine as a solvent, resulting in the selective formation of $[Al(Py)_4F_2]Cl$ (**2a**).

$$\underset{\mathbf{1a}}{AlCl_3 \cdot 3C_5H_5N} + 2Me_3SiF + n\mathrm{Py} \rightarrow \underset{\mathbf{2a}}{[Al(Py)_4F_2]Cl} + 2Me_3SiCl + (n-1)\mathrm{Py} \quad (1)$$

The solid-state structure of **2a** contains two terminal single Al−F-bonds within the helical *trans*-octahedron $[Al(Py)_4F_2]^+$-cation,[7] a building block still unique among the main group metals but found to be integral part of the structures of the few known neutral or charged difluoro-transition metal-pyridine complexes: $Os(Py)_4F_2$,[8] $Ni(Py)_4F_2 \cdot 2H_2O$,[9] $Cu(Py)_4F_2 \cdot 1.33HF \cdot 2H_2O$,[9] $Pd(Py)_4F_2 \cdot 1.5HF \cdot 2H_2O$,[10] $[Co(Py)_4F_2][H_2F_3]$[10] and $[Cr(Py)_4F_2][PF_6]$.[11]

In this study, we succeeded in the synthesis and characterization of two new complexes, $[Al(Py)_4F_2]Br \cdot$(**2b**) and $[Al(Py)_4F_2]I$ (**2c**). Furthermore, the reason for the incompleteness of the halogen exchange has found a quite plausible explanation after identification and characterization of the species undergoing the fluorination reactions. The thermal behavior of the most stable member **2a** was studied by TG and DTA. In addition, the reaction between **2a** and *cyclo-n*-propyl-phosphonic acid anhydride was investigated.

2. EXPERIMENTAL SECTION

General. All experiments were performed under a purified dry inert gas atmosphere (argon) in a glovebox and/or on glass high-vacuum line. Solvents were purified according to standard procedures and freshly distilled prior to use. The following chemicals were purchased from Aldrich: $AlCl_3$ (99.999%), $AlBr_3$ (99.999%), AlI_3 (99.999%), Me_3SiF (96%), phenyl phosphonic acid $PhP(O)(OH)_2$ (98%), and used without a further pretreatment. Trimeric *n*-propyl phosphonic acid cyclo-anhydride $[CH_3CH_2CH_2{-}PO_2]_3$ (50% by mass into ethyl

Received: July 16, 2012
Published: October 23, 2012

   dx.doi.org/10.1021/ic301502u | *Inorg. Chem.* 2012, 51, 11612−11622

acetate, Aldrich) was separated from the solvent by distillation and redissolved into pyridine just prior to use.

Methods. *X-ray Diffraction (XRD).* Measurements on powder samples were performed on a Seiffert RD3003TT (Freiberg, Germany) with Cu−Kα radiation. The moisture sensitive samples were prepared in a drybox, covered with a special X-ray amorphous polystyrene foil, and sealed by Kel-F grease (Roth).

Single Crystal XRD. Analysis was carried out on an IPDS diffractometer (Stoe & Cie) at 100 K using graphite-monochromated Mo-K_α (71.073 pm) radiation and cryostream cooler (Oxford Cryosystems). The moisture sensitive samples were fixed on the tip of a glass needle in a cold stream of nitrogen. The structures were solved[12] and refined[13] with the SHELTL program suite. Crystallographic data (excluding structure factors) for the structures reported in this paper have been deposited with the Cambridge Crystallographic Data Centre as supplementary publications no. CCDC-845758 for **2b**, CCDC-845759 for **2c**, CCDC-845760 for $[Al(Py)_4Br_2]Br{\cdot}0.5[PyH]Br{\cdot}(Py)$ (**3**) and CCDC-845761 for $[Al(H_2O)_4F_2]Cl{\cdot}2[PyH]Cl$ (**4**). Copies of the data can be obtained free of charge on application to CCDC (e-mail: deposit@ccdc.cam.ac.uk).

Solid-State NMR. spectra were recorded at room temperature on a Bruker Avance 400 spectrometer, operating at frequencies of 104.3 MHz for ^{27}Al, 161.9 MHz for ^{31}P and 376.4 MHz for ^{19}F. The MAS NMR measurements were performed using a 4 mm and a 2.5 mm double-bearing triple resonance (^{1}H/^{19}F−X) MAS probe (Bruker Biospin) at spinning rates between 12 and 15 kHz and between 25 and 30 kHz, respectively. The ^{27}Al MAS spectra were obtained using single pulse excitation with pulse durations of 1 μs (π/12 pulses). For a reliable signal-to-noise ratio the spectra were recorded by accumulating up to 72 800 scans with a recycle delay of 1s. To minimize line-shape distortions of the spectra caused by acoustic ringing and dead time of the MAS probe the first points (up to 32) of the FID were removed and an equal number, augmented of the points lost during the dead time previous acquisition, were reconstructed by using the backward linear prediction method. The ^{19}F MAS spectra were obtained using single pulse excitation consisting of 2 μs pulses (π/2 pulses) and recycle delays of 10 and 60 s to exclude saturation effects. Up to 128 FIDs were accumulated to obtain reliable signal-to-noise ratio. To suppress the strong background signal from the probe head, a phase-cycled depth pulse sequence according to Cory and Ritchey[14] was applied in addition to the above-mentioned single pulse sequence. The ^{31}P MAS spectra were measured using single pulse excitation with pulse durations of 4 μs (π/2 pulses). In order to avoid saturation effects a recycle delay of 180 s was used. Up to 500 scans were accumulated. The ^{27}Al, ^{31}P and ^{19}F spectra were externally referenced to 1 M aqueous $AlCl_3$ solution, to H_3PO_4 (85%) and to liquid $CFCl_3$ at 0 ppm, respectively.

The product of the reaction between $[Al(Py)_4F_2]Cl$ and the trimeric phosphonic acid anhydride $[CH_3CH_2CH_2{-}PO_2]_3$ was additionally studied by ^{31}P/^{27}Al TRAPDOR and ^{31}P−^{27}Al CP HETCOR experiments performed on a Avance 600 spectrometer (BAM, Berlin) equipped with a 4 mm double-bearing triple resonance (^{1}H−X−Y) MAS probe (Bruker Biospin). A MAS spinning rate of 12 kHz was used. The Lamor frequencies in these experiments were 242.9 MHz for ^{31}P and 156.4 MHz for ^{27}Al. The NMR parameters (chemical shifts, line widths, quadrupolar coupling constants) were fitted to the experimental spectra using the Topspin software (Bruker Biospin) and the dmfit[15] software package.

TG and DTA. measurements were performed using a NETZSCH thermoanalyzer STA 409 C *Skimmer* system. The experiments were carried out by applying a dynamic vacuum ($p < 10^{-2}$ mbar) or a constant purge gas flow of N_2 5.0 (Messer-Griesheim). A DTA-TG sample carrier system with Pt crucible and Pt/PtRh 10 thermocouples was used. Samples of 20−40 mg each were investigated by heating them from RT to 750 °C with constant rates of 1, 5, and 10 K/min or by their isothermal treatment till a constant mass at T_{iso} was observed.

Sample Preparation and Chemical Reactions. *$AlCl_3{\cdot}3Py$ (**1a**) and $AlBr_3{\cdot}3Py$ (**1b**).* Both molecular complexes were prepared from corresponding AlX_3 by adding 5−6 equivalents (stoichiometric excess) of pyridine and using benzene as a solvent. The purity of each compound was confirmed by elemental analysis (C, H, N, X), powder XRD and ^{27}Al MAS NMR. Attempts to crystallize **1b** from pyridine resulted in the formation of well shaped colorless crystals of compound $[Al(Py)_4Br_2]Br{\cdot}0.5[PyH]Br{\cdot}(Py)$ (**3**). The content of 0.5 mol [PyH]Br per formula unit in the lattice of **3** is due to hydrolysis of $AlBr_3$ by traces of water during the synthesis of **1b**.

*$AlI_3{\cdot}nPy$ (**1c**).* Four milliliters (49.7 mmol, 5.1 equiv) pyridine in 30 mL toluene were added slowly at 0 °C to 3.91g (9.6 mmol, 1 equiv) of AlI_3 dissolved into 40 mL of toluene. The reaction mixture was stirred at room temperature overnight. The precipitate was filtered, washed with cold pyridine and dried in vacuum. 4.35g of product **1c** was obtained, whose XRD powder pattern is almost identical with those reported for $AlI_3{\cdot}3Py$ (PDF No. 21−1859).[16,17] But except the conformation of XRD powder pattern our analytical data are at odds with the reported stoichiometry of 1:3. On the contrary, according to elemental analysis, **1c** does not contain the expected three but only two moles of pyridine: $(AlI_3{\cdot}2Py)$, $C_{10}H_{10}N_2AlI_3$ (MW 565.9) calcd C 21.24, H 1.77, N 4.95, found C 20.65, H 1.85, N 4.68; the calculated values for the reported[17−19] 1:3 complex $(AlI_3{\cdot}3Py)$ $[(C_{15}H_{15}N_3AlI_3)$ MW 645.0] are C 27.90, H 2.34, N 6.51.

*$[Al(Py)_4F_2]X$ (**2a−c**).* Compounds **1a−c** (5−10 mmol, 1.0 equivlent) were partially dissolved in pyridine (50 mL) in a 150 mL Schlenk tube. To the suspensions three to four equivalents of Me_3SiF were added at −20 °C within 2 h and the reaction mixtures additionally stirred at room temperature for 2 h. Me_3SiF excess was removed by pumping off. The precipitates formed as fine crystalline solids were filtered and recrystallized from hot pyridine. The resultant colorless pillar shaped crystals of compound **2a−c** were separated, washed with cold pyridine and dried in vacuum at room temperature. Yield: **2a** (72.5%),[7] **2b** (62.3%); $C_{20}H_{20}N_4AlF_2Br$ (MW 461.29) calcd. C 52.08, H 4.37, N 12.15, F 8.24; found C 51.48, H 4.12, N 11.22, F 7.85; **2c** (53.6%), $C_{20}H_{20}N_4AlF_2I$ (MW 508.28) calcd. F 7.48; found F 6 0.91; ^{19}F-NMR (Py-d5) δ: **2a**(−173.0),[7] **2b**(−172.5), **2c**(−172.2).

The chemical reactions with **2a** were performed by adding one equivalent of the above-mentioned reagents to its solutions or suspensions by using pyridine or methanol as a solvent.

3. RESULTS AND DISCUSSION

3.1. General Considerations. In 2006 we reported the synthesis and characterization of $AlF_2Cl{\cdot}4Py$, the first stable complex of a mixed aluminum halogen-fluoride in which the two fluorine atoms remain bound to the aluminum while the chlorine becomes substituted by pyridine forming a salt with the ionic structure $[Al(Py)_4F_2]Cl$ (**2a**).[7] On the contrary, in case of $AlCl_3{\cdot}nPy$ ($n \geq 3$) no such isomerization to the well-known analogous $[Al(Py)_4Cl_2]^+$-cation and chloride anion was observed. By X-ray single crystal[20] and powder[16] analysis we confirmed that the recrystallization of analytically pure **1a** from pyridine does not influence its neutral mononuclear molecular structure. The low melting point of **1a** (110 °C) is also in good agreement with its monomer molecular structure.[18] Thus, following eq 1 we assumed that after the substitution of two Cl-atoms in $AlCl_3{\cdot}3Py$ (**1a**) the hypothetical molecular complex $AlF_2Cl{\cdot}3Py$ is formed.[7] Unlike **1a** the later is transformed by pyridine into the ionic complex **2a**. Although the molecular nature of solid **1a** did not change after its isolation from pyridine, the true nature of the aluminum species present in the solution prior to and during the fluorination steps remains unknown. Conductivity data for pyridine solutions of $AlX_3{\cdot}3Py$ (**1a−c**) imply that ionic species should be present therein.[21] In attempts to crystallize **1b** from pyridine we obtained well shaped single crystals suitable for X-ray analysis. The determined structure showed not the expected 1:3 molecular complex **1b** but the compound **3**. It corresponds to the ionic complex $[Al(Py)_4Br_2]Br$ which crystallizes together with one solvent molecule and 0.5 pyridinium bromide in the lattice. The

isolation and structural characterization of **3** brought for the first time the proof that in pyridine solutions of **1a−c** solvated AlX_2^+-cations and X^--anions are present. Compound **3** is also the first example of a complex containing besides the halogens more than 3 molecules of pyridine directly coordinated at aluminum, thus, contradicting reports that compounds with stoichiometry greater than 3:1 do not occur within the $AlX_3 \cdot n$Py series.[17−19] For $AlX_3 \cdot n$Py (n = 1−3) with X = Cl, Br each compound was confirmed by X-ray powder diffraction analysis but in case of X = I only two of the three possible complexes, AlI_3·Py and AlI_3·3Py, were found. The existence of the 1:2-complex AlI_3·2Py was explicitly excluded.[17] Controversially to this report, the later complex is described by Gorenbein et al.[22] as a stable solid compound. Till now we were not able to obtain suitable single crystals of **1c** for crystal structure determination. The elemental analysis data do not support the reported 1:3 stoichiometry (see Experimental Section), but in view of the high moisture sensitivity of **1c** it was not possible to determine with certainty the correct chemical composition of the complex by elemental analysis. Our ^{27}Al solid state NMR measurements with **1c** samples, whose XRD powder patterns were almost identical to the reported for "AlI_3·3Py" (PDF No. 21−1859),[16] confirmed that **1c** is a phase pure compound with a solid state structure possessing only one $\sigma^4\lambda^3$-Al side. The dearth of reliable NMR data for AlI_3-compounds (see NMR section) do not allow at the present to distinguish between the possible two ionic structures $[Al(Py)_{1+x}I_{3-x}]xI$ (x = 1−2).

In view of the expected structural differences of **1a−c** we performed the reaction between one equivalent of **1b** or **1c** and 4−5 equivalents of Me_3SiF in pyridine. Unexpectedly, these reactions developed exactly in the same way as previously reported for the selective synthesis of **2a**.[7] The reactions proceed in accord to eq 1, leading in both cases to the exclusive formation of $[Al(Py)_4F_2]Br$ (**2b**) or $[Al(Py)_4F_2]I$ (**2c**), respectively. These findings support strongly the suggestion, that independent from the dissolved AlX_3 (X = Br, I) the dominated species in pyridine are very probably solvated AlX_2^+ - cations and solvated neutral molecules (AlX_3), doubly (AlX^{2+})- or triply charged (Al^{3+})-cations do not play a significant role. In case of **1a** the unchanged molecular complex was always isolated from the pyridine solutions and no formation of an ionic complex observed. However, the high selectivity in exchanging only two chlorines at **1a**, even by large excess of Me_3SiF, and the total absence of AlF_3 (cf. eq 1) can only be explained, if the dynamic equilibrium between 1:3-molecular and 1:4-ionic $AlCl_3$−pyridine complexes (eq 2) is inverted by the formation of Al−F-bonds (eq 3).

$$AlCl_3 \cdot 3C_5H_5N + n\,Py \rightleftharpoons [Al(C_5H_5N)_4Cl_2]^+ Cl^- + (n\text{-}1)Py \quad (2)$$

$$AlFCl_2 \cdot 3C_5H_5N + n\,Py \rightleftharpoons [Al(C_5H_5N)_4FCl]^+ Cl^- + (n\text{-}1)Py \quad (3)$$

3.2. Synthesis and Characterization of *trans*-Difluorotetrakis(pyridine)aluminum Salts. Multinuclear magnetic resonance spectroscopy was applied to characterize the powdered (polycrystalline) starting materials and the final products obtained by the described routes. In addition to their solid state NMR spectra, the new aluminum compounds have been characterized by the corresponding molecular structures as determined by single crystal X-ray analysis. For the well-characterized crystalline samples, the parameters of the ^{27}Al NMR spectra were precisely determined to discuss correlation between these parameters and details of the X-ray crystal structure. Such correlations will be useful for the interpretation of NMR spectra of amorphous aluminum halide phases.

3.2.1. ^{27}Al MAS NMR Characterization of AlX_3 (X = Br, I). The ^{27}Al MAS NMR spectra of the starting materials, pure polycrystalline $AlBr_3$ or AlI_3, are presented in Figures 1 and 2.

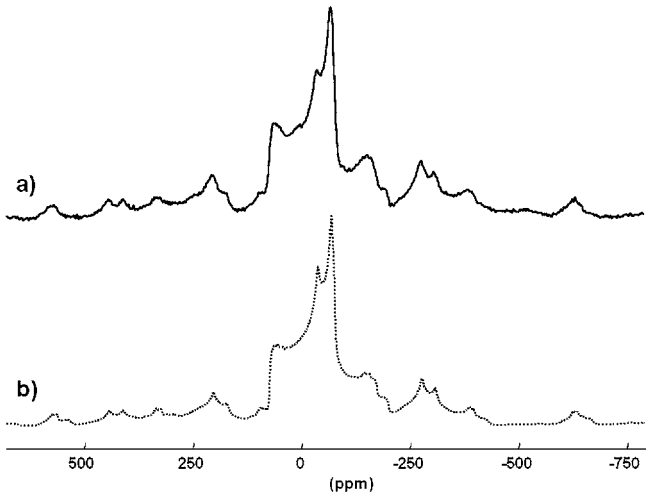

Figure 1. ^{27}Al MAS NMR spectrum of $AlBr_3$ measured with a spinning rate of 25 kHz: (a) experimental spectrum, (b) simulated central and satellite transitions with corresponding spinning sidebands.

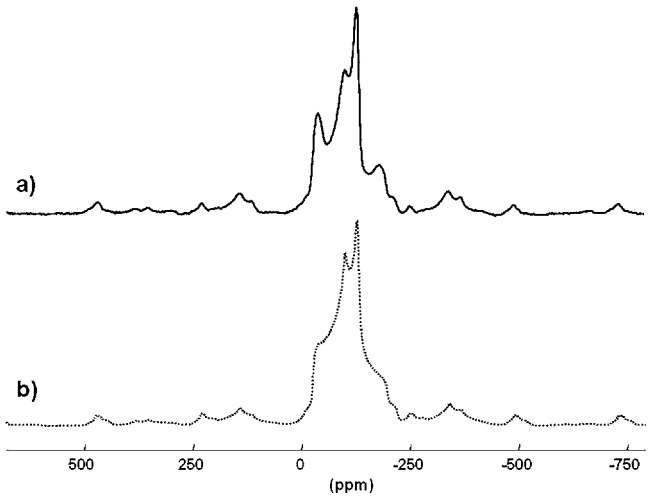

Figure 2. ^{27}Al MAS NMR spectrum of AlI_3 measured with a spinning rate of 25 kHz: (a) experimental spectrum, (b) simulated central and satellite transitions with corresponding spinning sidebands.

Both experimental spectra, obtained by applying a spinning speed of 25 kHz, show an unusual line shape due to a second-order quadrupolar interaction. The experimental spectra (a) are compared with the result of a line-shape analysis (b). Considering the existence of a single Al site in the respective structures, the central and satellite transitions with the corresponding spinning sidebands were simulated. The parameters of these simulations are summarized in Table 1. The experimental spectra of both compounds are depicted in Figures 1a ($AlBr_3$) and 2a (AlI_3). The spectra show a similar form of the line shape but differences in the position and the width of the shape. This similarity reflects the fact that both trihalides possess analogous structures. Indeed, their solid state structures are built up by molecular Al_2X_6 dimers as determined

dx.doi.org/10.1021/ic301502u | Inorg. Chem. 2012, 51, 11612−11622

Table 1. Results of the ^{27}Al MAS NMR Studies on Crystalline AlX_3, AlX_3·3Py and $[Al(D)_4F_2]X$ Compounds (D = Py and H_2O; X = Cl, Br and I)

	sample/cationic part	C.N.[a]	δ^b [ppm]	QCC[c] [kHz]	η^d	references
	$AlCl_3$	6	−1.4[e]	455[f]	0.34[f]	7
(**1a**)	$AlCl_3$·3Py	6	20.4[e]	847[g]	0.4[g]	7
(**2a**)	$[Al(Py)_4F_2]Cl/[Al(Py)_4F_2]^+$	6	3.6[f]	16070[f]	0.08[f]	7
(**4**)	$[Al(H_2O)_4F_2]Cl·2[PyH]Cl/[Al(H_2O)_4F_2]^+$	6	0.5[f]	9636[f]	0.27[f]	this study
	$AlBr_3$	4	76.4[f]	13500[f]	0.77[f]	this study
(**1b**)	$AlBr_3$·3Py	6	−2.2[e]	2300[g]	0.4[g]	this study
(**2b**)	$[Al(Py)_4F_2]Br/[Al(Py)_4F_2]^+$	6	3.8[f]	16201[f]	0.08[f]	this study
	AlI_3	4	−23.7[f]	11504[f]	0.71[f]	this study
(**1c**)	AlI_3·3Py	4	20.8[f]	8897[f]	0[f]	this study
(**2c**)	$[Al(Py)_4F_2]I/[Al(Py)_4F_2]^+$	6	3.4[f]	16232[f]	0.09[f]	this study

[a]Coordination number of the aluminum atom under study. [b]Isotropic ^{27}Al chemical shift. [c]Quadrupole coupling constant (= $e^2qQ/\hbar$) as a function of the electric quadrupole moment eq, the z-component, V_{zz} = eq, of the electric field gradient tensor and Plank's constant, $\hbar$. [d]Asymmetry parameter (= $(V_{xx} - V_{yy})/V_{zz}$) as a function of of the x, y and z components of the electric field gradient (EFG) tensor. [e]Measured value. [f]Calculated value. [g]Estimated value.

by X-ray single crystal analysis.[23−25] The Al_2X_6 units are characterized by a tetrahedral coordination of identical Al atoms bonded to two terminal (X1 and X2) and two bridging (X3 and X3′) halogens as schematically presented in Figure 3.

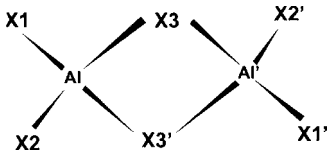

Figure 3. Schematic presentation of the structure of the dimeric Al_2X_6 molecules (X = Br, I).

The tetrahedral environments of the $\sigma^4\lambda^3$-Al atoms are distorted not only due to different four Al−X bond lengths but even more due to the X−Al−X angles that strongly deviate from the accurate tetrahedral angle of 109.5° with the largest values (120−122°) determined for the terminal and the smallest values (83−93°) for the bridging X atoms.[23−25] The relatively large values for the asymmetry parameter η (see Table 1) obtained from the line shape analysis for both compounds reflect these distortions. The deviations of the individual Br−Al−Br angles are larger than the I−Al−I angels in the corresponding solid structures.[23−25] That attends a larger electric field gradient and a larger QCC value for the Al nucleus in $AlBr_3$ as in AlI_3. Consequently, the central part of the experimental ^{27}Al MAS NMR spectrum of $AlBr_3$ is much broader compared with the corresponding spectrum of AlI_3. The performed line shape analysis resulted in a chemical shift value of 76.4 ppm for $AlBr_3$ and −23.7 ppm for AlI_3. Similar results were obtained by liquid state NMR studies. The measured ^{27}Al chemical shift values in different solvents are in a range between 77 and 79.6 ppm for the $[AlBr_4]^-$- anion and between −24 and −28 ppm for the corresponding $[AlI_4]^-$-anion.[26−28] NMR studies of aluminum compounds in solution have shown that the ^{27}Al chemical shifts are determined by two main factors: coordination number and the nature of the ligands.[29] Solid state ^{27}Al NMR studies confirmed these results. For a large number of oxygen coordinated aluminum compounds typical ranges for hexa-, penta- and tetra-coordinated aluminum have been obtained.[30] Furthermore, influences of the second coordination sphere on the ^{27}Al chemical shifts of oxygen coordinated aluminum were established and correlations between structural data and the ^{27}Al chemical shift values were reported.[31,32] Besides the oxygen coordinated aluminum compounds also such with other ligands have been studied by solid-state ^{27}Al NMR spectroscopy, among them halogen coordinated ones.

In this field, ^{27}Al NMR studies of pure fluorine coordinated aluminum in fluoroaluminates[33,34] and AlF_3-polymorphs[35] have been published. Whereas the aluminum in alkali fluoroaluminates and in all known AlF_3-polymorphs is without exception hexa-coordinated,[33,35] the existence of tetra-, penta- and hexa-coordinated Al species has been confirmed by a ^{27}Al NMR study of tetramethylammonium fluoroaluminates.[34]

Studies of mixed fluorine−oxygen coordinated aluminum in fluoride hydrates,[36] hydroxy fluorides[37] and isopropoxide fluorides[38] have shown that only in the later case besides the main hexa-coordinated (AlF_xO_{6-x}) compounds some penta-(AlF_xO_{5-x}) and tetra-coordinated (AlF_xO_{4-x}) units were additionally detected. Some few compounds with chlorine coordinated aluminum have also been studied by solid-state ^{27}Al NMR spectroscopy showing typical chemical shift ranges for tetra- (111.5−88 ppm), penta- (60−54.3 ppm) and hexa-coordinated aluminum (24.6 to −1.4 ppm).[7,39−41] Compared with the well-known ranges for oxygen coordinated aluminum the corresponding chemical shift values are more downfield shifted but reflect the same tendency: with increasing coordination number the corresponding chemical shift values become more high-field shifted.

Because there are no published solid state NMR data for bromine- and iodine-containing aluminum compounds for comparison, we can only consider here that the chemical shift of 76.4 ppm for $AlBr_3$ fits well in the known range of tertahedrally coordinated aluminum, whereas the value of −23.7 ppm for AlI_3 is unprecedented. It represents the most high field shifted value for a tetrahedrally coordinated aluminum in solids measured till now.

In order to find an explanation for the large differences in the chemical shift values of the tetrahydrally coordinated aluminum in the binary Al-halides $[AlCl_4]^-$ (101.4 ppm,[7] 100 and 103 ppm[39]), $(AlBr_3)_2$ (76.4 ppm) and $(AlI_3)_2$ (−23.7 ppm), we correlated these shifts with the improved electronegativity by Allred-Rochow for the corresponding ligands. Surprisingly, we obtained a linear correlation (R = 0.998) as shown in Figure 4. The electronegativity EN is a property that reflects the capability of an atom to withdraw the electrons within a covalent bond. The Cl atoms with the largest EN value attract

dx.doi.org/10.1021/ic301502u | Inorg. Chem. 2012, 51, 11612−11622

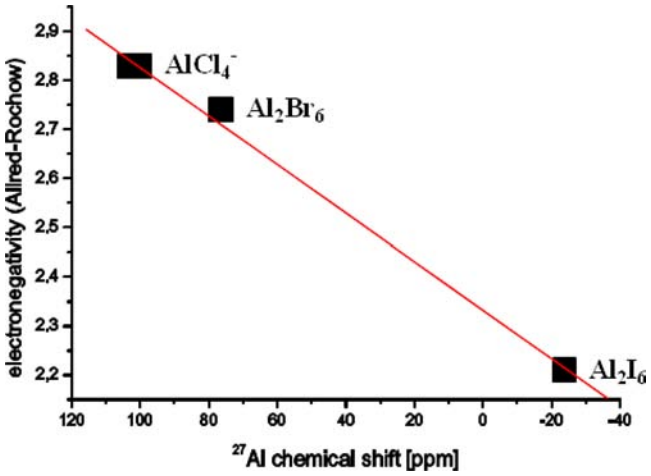

Figure 4. Correlation of the ^{27}Al chemical shifts of tetrahydrally coordinated aluminum in binary Al-halides with the improved electronegativity by Allred-Rochow for the corresponding ligands (■). The line represents the fitted linear correlation with a correlation coefficient R = 0.998.

the bonding electrons stronger than Br and I atoms, and as a result, the tetracoordinated aluminum nuclei ($\sigma^4\lambda^3$-Al) are most deshielded in $[AlCl_4]^-$, less in $AlBr_3$, and least in AlI_3.

3.2.2. ^{27}Al MAS NMR Characterization of AlX_3·3Py (X = Br, I). The ^{27}Al MAS NMR spectra for the bulk products resulting from the reaction of aluminum tribromide and triiodide with pyridine are presented in Figure 5 together with the corresponding spectrum of $AlCl_3$·3Py (**1a**) for comparison. Whereas the structure of **1a** is known and the octahedral coordination of aluminum well established, the structures of **1b** and **1c** are still unknown.[7,20] Our attempts to grow single crystals failed in both cases. Nevertheless, the information about the coordination sphere of aluminum in these compounds can be deduced from the presented NMR spectra. The ^{27}Al solid state NMR spectra of $AlBr_3$·3Py (**1b**) shows only one signal in the region characteristically for $\sigma^6\lambda^3$-Al. It is very broad compared to the corresponding signal of **1a**. Both are typical first-order quadrupolar spectra (Figure 5a and b) showing in each case only one resonance signal of nearly Gaussian line shapes due to the central transition of the aluminum nuclei and a set of the corresponding spinning sidebands caused by the satellite transitions. The spectra differ in the value of the chemical shift, the line width of the central signal and the number and the intensity distribution of the spinning sidebands as well. In both cases, the measured intensity distribution between the central signal and the spinning sidebands could not be simulated exactly so that only a raw estimation for QCC and η was possible.

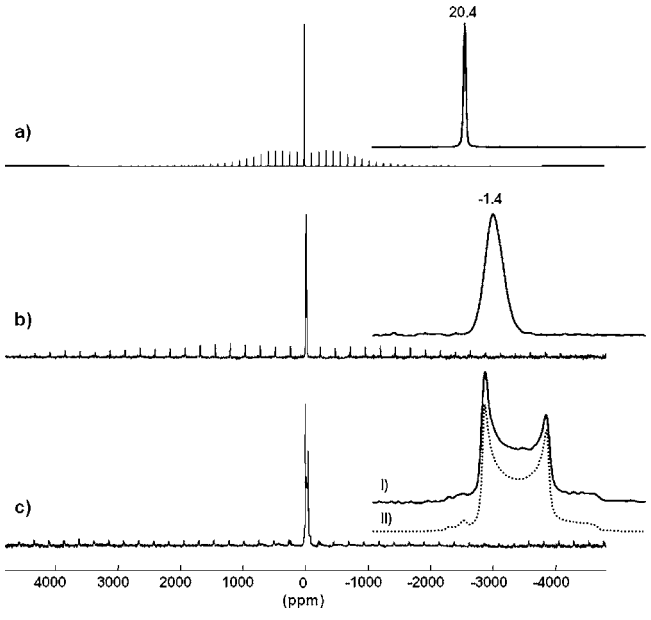

Figure 5. ^{27}Al MAS NMR spectra of AlX_3·3Py. (a) Experimental spectrum of $AlCl_3$·3Py measured with a spinning rate of 12 kHz, (b) experimental spectrum of $AlBr_3$·3Py measured with a spinning rate of 25 kHz, (c) experimental spectrum of AlI_3·3Py measured with a spinning rate of 25 kHz. The insets show the central parts of the corresponding spectra in the same scale. In (c) the experimental spectrum (I) is compared with the result of the simulation (II) taking into account the central and satellite transitions.

In contrast to the ^{27}Al MAS MNR spectra of **1a** and **1b**, the corresponding spectrum of **1c** ("AlI_3·3Py") shows a central signal with a typical line shape due to second-order quadrupolar interaction (Figure 5c). The values for the isotropic chemical shift, QCC and η, were calculated by performing a line shape analysis. The resulting theoretical line shape (Figure 5c, insert II) shows the high accuracy of this analysis. The parameters of all three spectra are summarized in Table 1.

The observed single NMR signal in each spectrum demonstrates the existence of only one crystallographic site for aluminum in both structures (**1b**, **1c**), as it was determined for **1a**.[7]

Comparing the isotropic ^{27}Al chemical shift values for $AlBr_3$ and $AlBr_3$·3Py a drastic jump from 76.4 ppm for the starting compound to −1.4 ppm for the final product **1b** was observed. This high field shifting can only be explained by a change in the coordination sphere of aluminum in the corresponding structures: from a tetrahedrally coordination in $(AlBr_3)_2$ to an octahedrally coordination in $AlBr_3$·3Py. For oxygen and chlorine coordinated aluminum atoms the correlation between chemical shift and coordination number is known and therefore it is assumed that it is valid for bromine coordinated aluminum, too. Thus, our NMR studies suggest a similar structure for $AlBr_3$·3Py (**1b**) as observed in $AlCl_3$·3Py (**1a**), a molecular structure with a single crystallographic site of a 6-fold coordinate aluminum by three halogens and three pyridines.

The larger QCC of **1b** compared with the corresponding value of **1a** points to the existence of a higher electric field gradient. The much broader line width of the resonance signal in the spectrum of the bromine complex is caused either by this larger QCC or probably by a poor crystallinity of the **1b** samples compared with the studied samples of **1a**.

The comparison of the isotropic ^{27}Al chemical shift values between $(AlI_3)_2$ and "AlI_3·3Py" shows a change to lower fields from −23.7 ppm for the starting compound to 20.8 ppm for the final product. In our studies of $AlCl_3$−pyridine complexes, we found that a substitution of chlorine by pyridine in the first coordination sphere of aluminum leads to a low-field shift of the ^{27}Al chemical shift for tetrahedrally as well as for octahedrally coordinated aluminum.[7] We observed the same trends for both complexes **1b** and **1c**. While the high-field shift in going from $(AlBr_3)_2$ to $AlBr_3$·3Py indicates the change in the coordination sphere of aluminum from $\sigma^4\lambda^3$-Al to $\sigma^6\lambda^3$-Al, the low-field shift in case of the triiodide system clearly demonstrates only a substitution of iodine by pyridine without

dx.doi.org/10.1021/ic301502u | Inorg. Chem. 2012, 51, 11612−11622

changing the aluminum coordination number. The comparison of QCC and η shows smaller values for "$AlI_3 \cdot 3Py$" which means that the mixed iodine-pyridine coordination in "$AlI_3 \cdot 3Py$" generates a smaller and more symmetric electric field gradient at the $\sigma^4\lambda^3$-Al center as in case of the pure iodine coordinated aluminum in $(AlI_3)_2$.

Unfortunately, our NMR results do not allow deducing information about the number of the substituted iodine by pyridine without the knowledge of the exact structure.

3.2.3. ^{27}Al MAS NMR Characterization of $[Al(Py)_4F_2]X$ (X = Br, I). The ^{27}Al MAS NMR spectra of the crystalline reaction products obtained by the reaction of **1b** and **1c** with Me_3SiF in pyridine, are presented in Figures 6 and 7. The experimental

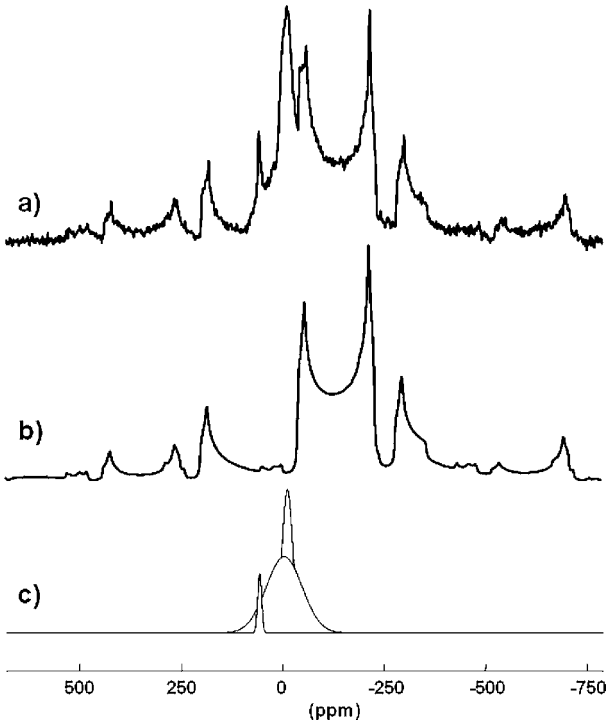

Figure 6. ^{27}Al MAS NMR spectrum of $[Al(Py)_4F_2]Br$ (**2b**) measured with a spinning rate of 25 kHz: (a) experimental spectrum, (b) simulated central and satellite transitions with corresponding spinning sidebands, (c) aluminum-containing byproducts.

spectra (a), obtained by applying a spinning speed of 25 kHz, are compared with the result of a line-shape analysis (b) in which the central and satellite transitions with the corresponding spinning sidebands were simulated, taking into account the existence of only one Al site in the structure of both compounds. The parameters of these simulations are summarized in Table 1. To simulate the corresponding experimental spectra completely, a few small symmetric lines were added (c) which point to the existence of aluminum containing byproducts with unknown structures and compositions.

The cation $[Al(Py)_4F_2]^+$ is the essential part of **2b** and **2c** and was already characterized by solid-state NMR spectroscopy in case of $[Al(Py)_4F_2]Cl$.[7] We demonstrated that the extremely large value of the QCC is caused by an extreme shortening of the aluminum-halogen distances occurring during the substitution of chlorine by fluorine so that the formed cation $[Al(Py)_4F_2]^+$ consists of two explicitly shorter Al−F bonds compared with the four Al−N bonds. The same structural

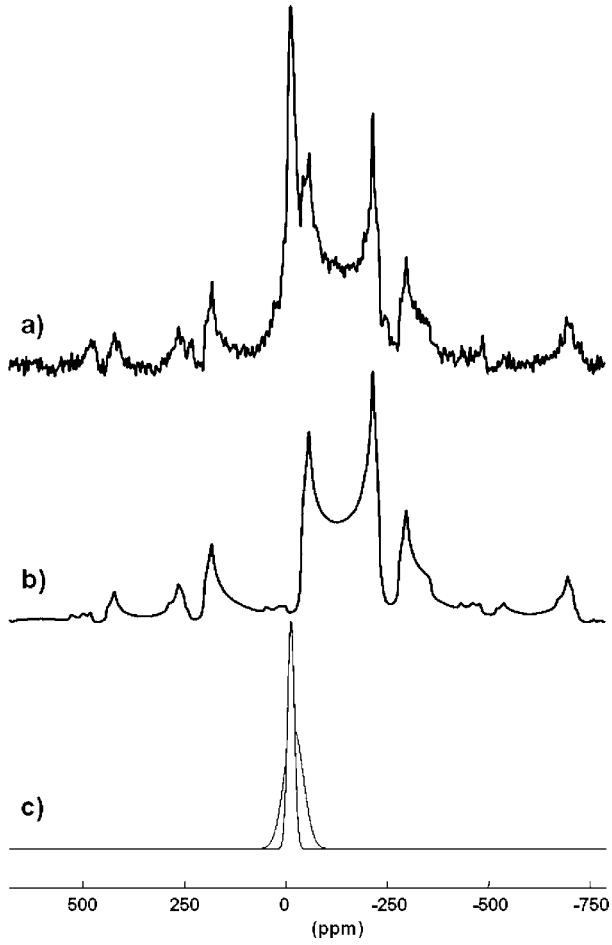

Figure 7. ^{27}Al MAS NMR spectrum of $[Al(Py)_4F_2]I$ (**2c**) measured with a spinning rate of 25 kHz: (a) experimental spectrum, (b) simulated central and satellite transitions with corresponding spinning sidebands, (c) aluminum-containing byproducts.

feature was obtained for the cation of $[Al(Py)_4F_2]Br$ and of $[Al(Py)_4F_2]I$, too (see Table 3). The comparison of the calculated chemical shift, QCC and η (see Table 1) for all three compounds (**2a**, **2b**, **2c**) obtained by the line-shape analysis show analogous data. The differences in the QCC values are less than 1% and the calculated chemical shift differ only by 0.4 ppm which are within the limits of reproducibility. Therefore, the NMR studies show that an influence of the anion on the structure of the cation $[Al(Py)_4F_2]^+$ is not detectable in any case of the three compounds (**2a**, **2b**, **2c**).

3.2.4. Crystal Structures. The crystallographic data obtained from the X-ray diffraction investigations for all four new compounds are summarized in Table 2. In Table 3, selected bond lengths and angles for **2b** and **2c** are given and the data of **2a** included for comparison. The measured bond lengths and angles in $[Al(Py)_4F_2]^+$ - cations of **2b** and **2c** are nearly identical with the corresponding values found in **2a**, showing only a negligible influence of the halogen anions on the solid structures. These findings are in perfect agreement with the results derived from the solid state NMR investigations mentioned above.

The cationic part $[Al(Py)_4Br_2]^+$ of compound **3** is presented in Figure 8, together with some relevant bond lengths and angles. $[Al(Py)_4Br_2]^+$ represents only the forth example within CSD Databank of a structural fragment having at least one

dx.doi.org/10.1021/ic301502u | *Inorg. Chem.* 2012, 51, 11612−11622

Table 2. Crystal Structure Information for $[Al(Py)_4F_2]Br$ (2b); $[Al(Py)_4F_2]I$ (2c); $\{[Al(Py)_4Br_2]Br{\cdot}0.5[PyH]Br{\cdot}(Py)\}_2$ (3) and $[Al(H_2O)_4F_2]Cl{\cdot}2[PyH]Cl$ (4)

compound	2b	2c	3	4
formula	C_{20} H_{20} Al Br F_2 N_4	C_{20} H_{20} Al I F_2 N_4	$C_{55}H_{56}$ Al_2 Br_7N_{11}	$C_{10}H_{20}AlCl_3F_2$ N_2O_4
Fw /(g/mol)	461.29	508.28	1484.44	403.61
crystal system	monoclinic	monoclinic	monoclinic	monoclinic
space group (no.)	*C*2/*c* (15)	*C*2/*c* (15)	$P2_1/c$ (14)	$P2_1/m$ (11)
crystal size/mm	0.30; 0.24; 0.20	0.28; 0.24; 0.18	0.6; 0.543; 0.48	0.20; 0.10; 0.09
a/Å	14.8509(5)	15.1899(16)	9.3388(2)	5.0967(3)
b /Å	11.8375(4)	12.2837(14)	23.5193(7)	19.7672(11)
c /Å	12.9196(4)	13.0435(14)	13.2184(3)	9.0423(7)
β /deg	118.869(2)	119.816(7)	90.124(2)	103.089(6)
V/Å^3	1988.98(11)	2111.6(4)	2903.31(13)	887.32(10)
ρ_{calc} /g cm^{-3}	1.540	1.599	1.698	1.511
Z	4	4	2	2
μ (Mo-K*α*)/mm^{-1}	2.142	1.588	4.914	0.600
2Θ − range/deg	4.66−58.26	4.74−58.24	4.36−54.40	4.62−55.00
reflns (total/indep)	15503/2678	12316/2825	45124/6338	18004/2105
R_{int}	0.0583	0.1164	0.1722	0.0996
reflns, $I > 2\sigma(I)$	2348	2554	5845	1799
reflections/params	2678/129	2825/129	6428/349	2105/170
$R1^a$ $[F_0 > 4\sigma(F_0)]$	0.0322	0.0549	0.0758	0.0388
$wR2^b$ (all data)	0.0660	0.1134	0.1852	0.0810
GoF (all data)	1.081	1.216	1.269	1.085
ρ_{final}(max/min) /eÅ^{-3}	0.397/-0.373	2.055/-2.116	2.196/-2.612	0.314/-0.338

$^a R1 = \Sigma\ ||F_o| - |F_c||/\Sigma\ |F_o|$. $^b wR2 = [\Sigma\ w(F_o^2 - F_c^2)^2/\Sigma\ w(F_o^2)^2]^{1/2}$.

Table 3. Selected Bond Lengths (pm) and Angles (deg) in $[Al(Py)_4F_2]X$ for X = Cl (2a),[7] Br (2b), I (2c)

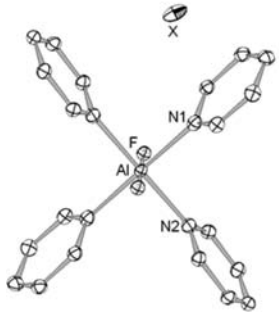

	compound		
	2a	2b	2c
Al – F	171.94(6)	171.91(9)	172.4(2)
Al – N1	206.83(9)	206.83(14)	207.5(4)
Al – N2	207.69(9)	208.01(14)	208.4(3)
F – Al – N1	90.37(3)	90.24(5)	90.22(13)
F – Al – N2	90.09(3)	89.76(5)	90.44(13)
N1 – Al – N2	92.63(3)	87.29(5)	92.31(14)

bromine atom bonded directly to a 6-fold coordinated aluminum center, besides a neutral complex of $AlBr_3$ with the 3-fold O-donor ligand $(CH_3O{-}C_2H_4{-}O{-}C_2H_4{-}OCH_3)$[43] and two ionic compounds $([Al(CH_3CN)_5Br]{\cdot}2[AlBr_4]{\cdot}CH_3CN)$.[44] and $([Al(THF)_4Br_2][AlBr_4]{\cdot}C_6H_6{\cdot}CH_3C_6H_5)$.[45] The Al−Br distances in $[Al(Py)_4Br_2]^+$ with 249.3 and 249.8 pm are longer than the Al−Br bonds at the comparable *trans*-$[Al(THF)_4Br_2]^+$ cation with 243.7 pm. The four pyridine ligands are oriented propeller blades like across the central Al atom defining by slightly different four Al−N bonds the equatorial AlN_4 plane of $[Al(Py)_4Br_2]$-octahedron. The strong distortion of the later is mostly caused by the much longer distances of aluminum to both Br atoms standing in *trans* position to each other. In comparing the geometrical parameters of the three structurally characterized *trans*-$[Al(Py)_4X_2]^+$ cations (X = F,[7] Cl,[20] Br) we recognize the same bonding motifs defined by octahedral environment of the central Al atom with nearly equal equatorial Al−N bond lengths of 203.4− 207.6 pm but very different Al−X axial distances.

For the recording of the ^{27}Al MAS spectra of compound **3** a few single crystals have been crushed under inert conditions and the resulted powder was packed into a 2.5 mm rotor. On the one hand, the obtained spectrum (not shown here) consists of a single signal at −0.2 ppm which is downfield shifted compared with the corresponding signal of **1b** at −2.2 ppm. The formal substitution of bromine by pyridine in the first coordination sphere of aluminum shows even in this case the expected shift to lower field. On the other hand, the line-shape of the signal shows an extremely anisotropic broadening and low intensities of the spinning sidebands. Because both facts are not expected for well-crystalline samples, we can not exclude that compound **3** undergoes changes during the sample preparation and/or the NMR measurement, probably loosing its former crystallinity. Therefore, the obtained NMR results for **3** are not included in Table 1.

3.4. Thermal Analysis Study and Chemical Reactions of 2a. We already reported the formation of *η*-AlF_3 by the thermal decomposition of **2a** at 455 °C under dynamic vacuum conditions ($p < 10^{-2}$ mbar).[35] Depending on the performed cooling regime, we obtained products of a varying phase purity:

dx.doi.org/10.1021/ic301502u | *Inorg. Chem.* 2012, 51, 11612−11622

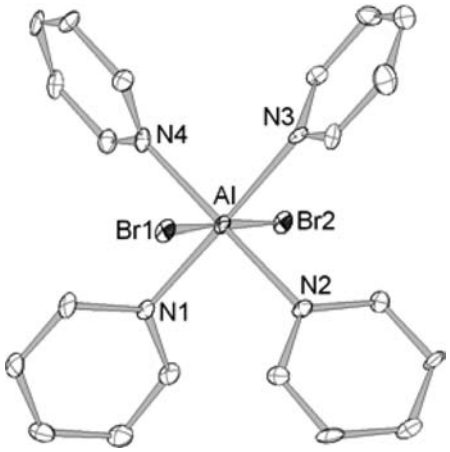

Figure 8. Crystal structure of the cationic part $[Al(Py)_4Br_2]^+$ of compound **3** $[Al(Py)_4Br_2]Br{\cdot}0.5[PyH]Br{\cdot}(Py)$ (DIAMOND,[42] the ellipsoids represent a 50% probability; for clarity, H atoms are not shown, C atoms are not labeled). Selected bond lengths [pm]: Al–Br(1) 249.8 (2), Al–Br(2) 249.3(2), Al–N(1) 204.3(6), Al–N(2) 203.4(7), Al–N(3) 205.2(6), Al–N(4) 207.6(7), and angle [deg]:Br(1)–Al-Br(2) 177.7(1).

cooling down slowly led to "XRD pure" η-AlF_3 but the sudden quenching from 455 °C to room temperature left a powder which showed additional reflections in its XRD pattern.[35] These findings prompted us to study once again the thermal behavior of **2a**. The solid decomposition products leaving the system by sublimation as well as the remaining powders were analyzed by X-ray and solid state NMR. TG and DTA measurements showed three characteristic regions between room temperature and 750 °C for the decomposition of **2a**: the first one (up to ca. 350 °C) is characterized by pyridine loss and the continuous formation of $AlCl_3$–pyridine complexes. The later are descended from not jet identified aluminum chlorine-fluorine intermediates by dismutation reactions and they go out of the system by sublimation as proved by ^{27}Al-MAS NMR. No useful information can be extracted from the ^{27}Al, ^{19}F and ^{1}H solid state NMR and XRD investigations on the remaining powder at this stage. The spectra showed very wide and overlapped lines confirming only the XRD amorphous character of the samples. In addition small amounts of $[C_5H_5NH]^+$ salts with Cl^- and/or $[AlCl_4]^-$ anions due to hydrolysis by traces of moisture were detected by ^{27}Al NMR. In the second temperature range (350–500 °C) a mass loss of about 10% takes place which is directly linked with the formation of η-AlF_3. After the constant mass of the sample is reached at ca. 500 °C we observed always the "pure XRD pattern" of η-AlF_3 without any influence by the cooling down regime. Thus, the previously reported dependence of the later on the phase purity of η-AlF_3 does not exist and the observed unknown reflections at that time were probably from not fully removed "volatiles" after the sudden quenching of the samples.[35] The third temperature range (starting at ca. 500 °C) represents the thermal behavior of the pure η-AlF_3: it is characterized by two exothermal effects with maxima at 621 and 697 °C indicating the two step phase transition of η-AlF_3 over β-AlF_3 to the final modification α-AlF_3 as proved by XRD and NMR measurements. A similar consecutive cascade of phase transformations of η-AlF_3 (400 °C) over θ-AlF_3 (500 °C) and β-AlF_3 (600 °C) to α-AlF_3 was observed by our studies on the thermal behavior of ACF.[2] It should be pointed out that η-AlF_3 can not be obtained phase pure by the thermolysis of ACF.[35] TA-MS curves for "XRD-pure" η-AlF_3, prepared from **2a**, in argon flow coupled with ion current curves for the mass numbers m/z = 18 (H_2O^+) and 44(CO_2^+) showed surprisingly that the collapse of the channel structure during the transition of β-AlF_3 to α-AlF_3 does not liberate H_2O but is accompanied by release of CO_2.

The hydrolysis of **2a** by water or diluted hydrochloric acid precipitated the well-known $AlF_2(OH)$ compound of pyrochloric structural type as shown by elemental analysis, XRD (pdf 11–631),[16] and NMR (^{19}F, ^{27}Al) analysis. However, if the hydrolysis is performed carefully in methanol by very diluted hydrochloric acid, after slowly evaporation of the solvent and annealing the solid at 60 °C in argon flow, besides powdered $AlF_2(OH)$ as the main product few single crystals developed. The later were separated manually in a drybox using a microscope with polarizing light and analyzed by XRD single crystal analysis and solid state NMR (^{19}F, ^{27}Al). The performed X-ray diffraction investigations resulted in the structure determination of the new compound $[Al(H_2O)_4F_2]Cl{\cdot}2[PyH]$-Cl (**4**). The structure of compound **4** is very closely related to the previously reported structure of $[Al(Py)_4F_2]Cl{\cdot}2[PyH]Cl$ identified among the hydrolysis products of $[Al(Py)_4F_2]Cl$ in pyridine .[7] The crystallographic data of **4** are shown in Table 2. The most prominent feature of the structure of compound **4** is the presence of $[Al(H_2O)_4F_2]^+$-cations which are interconnected over O–H···F hydrogen bonds forming this way a "band-like" structural motif. An arrangement of two F and four H_2O ligands in the first coordination sphere of a center has been determined for the first time among the main group metals and it is besides the reported structure of $[Ti(H_2O)_4F_2]^+$ only the second example in literature.[46] Selected bond lengths and angles for the $[Al(H_2O)_4F_2]^+$-cation are shown in Figure 9.

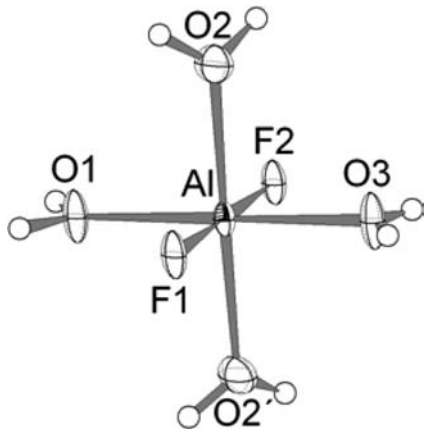

Figure 9. Crystal structure of the cationic part $[Al(H_2O)_4F_2]^+$ of compound **4** $[Al\ (H_2O)_4F_2]Cl{\cdot}2[PyH]Cl$ (DIAMOND,[42] the ellipsoids represent a 50% probability, for clarity, H-atoms are not labeled). Selected bond lengths [pm]: Al–F(1) 174.72(16), Al–F(2) 174.96(16), Al–O(1) 189.44(17), Al–O(2) 191.65(15), Al–O(3) 188.55(17) and angle [deg]: F(1)–Al-F(2) 179.43(7).

In addition this cation was characterized by ^{27}Al and ^{19}F MAS NMR spectroscopy. The spectroscopic studies were performed on samples prepared from the collected single crystals. Crystallites were first crushed and the powdered samples packed into a 2.5 mm rotor. All handlings were performed in a glovebox under argon atmosphere. Figure 10 represents the central part of the experimental ^{27}Al NMR spectrum (a),

dx.doi.org/10.1021/ic301502u | Inorg. Chem. 2012, 51, 11612–11622

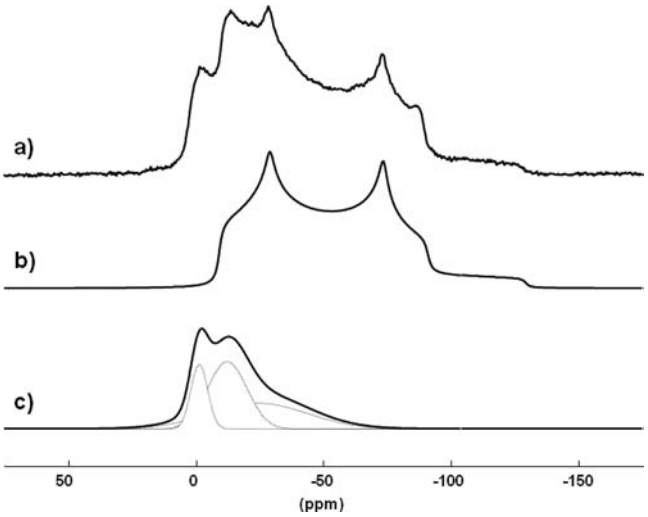

Figure 10. ^{27}Al MAS NMR spectrum of $[Al(H_2O)_4F_2]Cl{\cdot}2[PyH]Cl$ (**4**) measured with a spinning rate of 25 kHz: (a) experimental spectrum, (b) simulated central transition, (c) byproduct attributed to $AlF_2(OH)$ pyrochlore.

obtained by applying a spinning speed of 25 kHz, compared with the result of a line-shape analysis (b) in which only the central transition was simulated under consideration that a single Al site exists. The parameters of this simulation are summarized in Table 1. To simulate the corresponding experimental spectra completely, three small symmetric lines of a Gaussian line-shape were added (dotted lines in c). The solid line in (c) represents the superposition of the three Gaussian lines. The resulted line-shape shows a close similarity to the measured ^{27}Al MAS NMR spectra at 9.6T of $AlF_{3-x}(OH)_x$ pyrochlore[36] and reproduces nearly the same chemical shift values as the ^{27}Al NMR spectrum of the $AlF_2(OH)$ pyrochlore, obtained by hydrolysis of $[AlF_2(Py)_4]Cl$ with HCl/H_2O. Therefore, we suppose that the studied sample consists of two compounds, $[Al(H_2O)_4F_2]Cl$ (**4**) as the main compound (~70%) and $AlF_2(OH)$ pyrochlore as a byproduct (~30%), both formed by the hydrolysis of **2a**. This assumption is confirmed by the result of the ^{19}F NMR measurement. The NMR spectrum in Figure 11 shows two resolved lines with an intensity ratio of about 70:30, the same ratio as obtained from the ^{27}Al NMR spectrum. Therefore, the most intense signal at

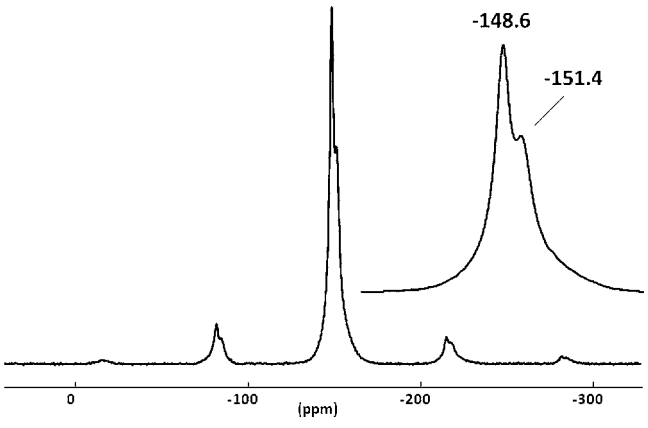

Figure 11. Experimental ^{19}F MAS NMR spectrum of $[Al(H_2O)_4F_2]$-$Cl{\cdot}2[PyH]Cl$ measured with a spinning rate of 25 kHz. The inset shows the central part of the spectrum in an enlarged scale.

−148.6 ppm is attributed to the fluorine in $[Al(H_2O)_4F_2]Cl$, the signal at −151.4 ppm to the fluorine in $AlF_2(OH)$ pyrochlore. For the bulk product obtained by the hydrolysis of **2a** with HCl/H_2O we have measured a ^{19}F NMR signal at −152.5 ppm but with a line-width four times broader as in the case described above.

A comparison of the NMR data for $[Al(H_2O)_4F_2]Cl$ with the corresponding values for $[Al(Py)_4F_2]Cl$ (**2a**) shows more or less significant changes (see Table 1). These changes are caused by structural modifications of the cation as a result of pyridine replacement by water and the formation of hydrogen bonds.

The drastic reduction of the QCC from 16 MHz in (**2a**) to 9.6 MHz in (**4**) can be explained by the fact that the differences between the Al−F and Al−O bond lengths in (**4**) became much smaller than the differences in the corresponding bond lengths (Al−F and Al−N) in (**2a**). This resulted in a smaller electric field gradient and, consequently, its interaction with the electric quadrupole moment of the Al nucleus induces a smaller value of the QCC compared with the values obtained for **2a**. The increase in the value of the asymmetry parameter η from 0.08 in **2a** to 0.27 in **4** expresses the fact that the cation in **4** exhibits a lower symmetry than the cation in **2a**. Both pseudo C2 axes of rotation defined by exchanging the fluorine positions in **2a** are probably quashed by the protons of water in **4**. The change of the isotropic chemical shift of **4** by about 3 ppm to a higher field as compared to **2a** is caused by the substitution of pyridine by water in the coordination sphere of aluminum. This means that in this case water leads to a stronger shielding of the aluminum nucleus than pyridine.

Our attempts to develop a reproducible synthesis for compound **4** by the controlled hydrolysis of **2a** were not yet successful. Also the performed chemical reactions with **2a** aiming at the efforts to find out a synthesis approach for introducing the AlF_2-group into different organic compounds were not yet crowned with success. From the plenty of experiments in reacting **2a** with CH_3CH_2OH, CF_3CH_2OH, $(CH_3)_2CHOH$, $(CF_3)_2CHOH$, $Li\{Al[OCH(CF_3)_2]_4\}$, $AgOOCCF_3$, Ph-P(O)$(OH)_2$ and *cyclo*-n-propyl-phosphonic acid anhydride, only the results of the last reaction are presented very briefly. It was expected to introduce the AlF_2-group into "the phosphonate end" of the triphosphonic backbone by opening the *cyclo*-$[CH_3CH_2CH_2{-}PO_2]_3$ with the formation of the hypothetical acid chloride $(Py)_x$ F_2 Al−O−P(O)(R)O−P(O)(R)O−P(O)(R)Cl ($x \leq 3$). The characterization of the obtained product by solid-state NMR revealed an unexpected course of the performed reaction. The ^{27}Al MAS NMR experiment results in a typical first-order quadrupolar spectrum with a narrow signal at −18.4 ppm showing the completed reaction of $[Al(Py)_4F_2]Cl$ to a new product. The completeness of the reaction is also confirmed by the ^{19}F MAS NMR spectrum. It shows only a new signal at −67.3 ppm which is typical for fluorine directly bonded to phosphorus and there are no any indications for the presence of Al−F bonds in the sample.

Thus, the ^{19}F MAS NMR spectrum reveals an unexpected course of the reaction which is accomplished by the total fluorine migration from aluminum to phosphorus. Therefore, the value of −18.4 ppm in the ^{27}Al MAS NMR spectrum of the product points to the existence of octahedrally coordinated aluminum which does not contain any fluorines in the first coordination sphere. Studies of aluminophosphate glasses of different compositions showed similar chemical shift values (−10 to −15 ppm) for the aluminum−phosphorus connectivity

in the corresponding glass network units[47−49] and the most high-field shift at −21.6 ppm was determined for such structural units in crystalline $Al(PO_3)_3$.[50]

In accord with this, our product contains aluminum, which is very probably coordinated by oxygen in the first and phosphorus in the second coordination sphere.

The ^{31}P MAS NMR spectra were of low resolution as expected for amorphous samples. The line-widths were in order of 2 kHz and showed only the incorporation of different phosphorus atoms without a significant contribution for structural proposals. On the basis of these results it was impossible to distinguish between a uniform compound or a mixture of different phases. Therefore, we applied $^{27}Al-^{31}P$ double resonance techniques to characterize the existing connectivities between aluminum and phosphorus in the studied sample.

The result of a $^{31}P/^{27}Al$ TRAPDOR experiment is presented in Figure 12. Spectrum (a) shows the ^{31}P MAS NMR spectrum

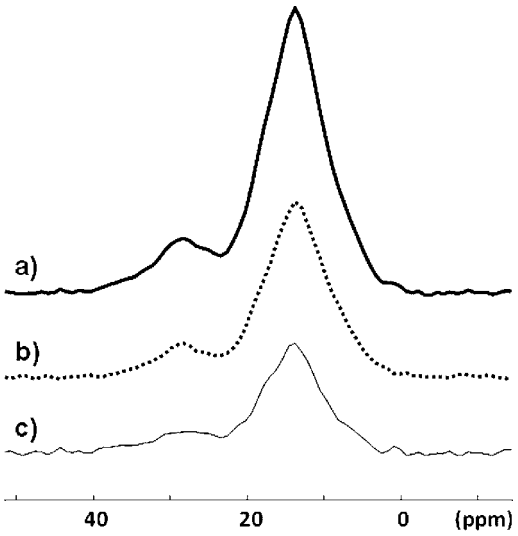

Figure 12. $^{31}P-^{27}Al$ TRAPDOR results of the reaction product of **2a** with phosphonic acid anhydride: (a) spectrum acquired without irradiation of the ^{27}Al nuclei, (b) spectrum acquired with irradiation of the ^{27}Al nuclei and (c) difference spectrum ΔS.

obtained with a rotor-synchronized Hahn-Echo (τ = 4.08 ms) and a spinning rate of 12.5 kHz without Al irradiation in the second channel. Spectrum (b) was acquired under the same conditions but with an irradiation to the ^{27}Al nuclei. The difference spectrum ΔS is depicted in (c). A comparison of (a) and (b) shows that the effect of the ^{27}Al irradiation during the TRAPDOR experiment influences the signal and the shoulder of the ^{31}P MAS NMR spectrum in the same manner indicating that all phosphorus environments are affected by the ^{27}Al dipolar coupling. This suggests that aluminum is connected with all kind of different phosphorus atoms.

In order to differentiate between connectivities of aluminum and phosphorus atoms two-dimensional $^{27}Al\rightarrow^{31}P$ CPMAS HETCOR experiments were performed. The two-dimensional $^{27}Al\rightarrow^{31}P$ CPMAS correlation spectrum is shown in Figure 13. Intensity in the two-dimensional contour map indicates proximity between the corresponding ^{27}Al and ^{31}P nuclei. We derive the same result as mentioned above. The aluminum is bonded to every of the different phosphorus atoms.

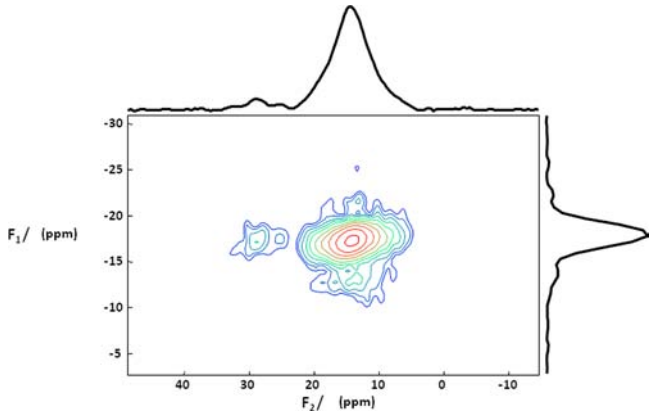

Figure 13. Two-dimensional $^{27}Al\rightarrow^{31}P$ CPMAS HETCOR spectrum of the reaction product of **2a** with phosphonic acid anhydride.

Summarizing the result of the applied NMR techniques we can consider that the reaction product can be described as a uniform compound consisting of octahedrally coordinated aluminum with oxygen in the first and phosphorus in the second coordination sphere. Fluorine coordinated aluminum does not exist and all fluorine atoms are bonded directly to phosphorus.

Unfortunately, the constitution and the structure of the compound remain still unknown.

4. CONCLUSIONS

Crystalline $AlBr_3$, AlI_3 as well as their "pyridine richest" complexes isolated from the respective pyridine solutions at large stoichiometric excesses of pyridine (**1b** and **1c**) were studied for the first time by ^{27}Al solid state NMR spectroscopy. The data obtained concern the analysis of chemical shift ranges and the determination of the quadrupole coupling constants providing useful contributions to the characterization of these solid compounds in order to determine the coordination number of Al atom in the various environments. Thus, the reported 1−3 stoichiometry for $AlBr_3{\cdot}3Py$ (**1b**) was confirmed by solid state NMR, showing the Al atom in the expected octahedral coordination. On the contrary, the solid state NMR results do not support the reported 1 to 3 stoichiometry for the corresponding complex $AlI_3{\cdot}3Py$ (**1c**), showing clearly the Al atom in a tetrahedral coordination. Fluorination studies of these complexes using Me_3SiF as a fluorinating agent aimed at the successful synthesis of $[Al(Py)_4F_2]X$ (X = Br, I) as previously reported for the corresponding complex $[Al(Py)_4F_2]Cl$.[7]

In pyridine solutions of AlX_3, one Al−X covalent bond undergoes predominantly homolytic cleavage by the solvent molecules forming solvated AlX_2 cations as the major species. Thus, prior to or during fluorination steps, only the remaining two covalent Al−X bonds are accessible to X/F-exchange, a fact that favors the selective formation of $[Al(Py)_4F_2]X$ (X = Cl, Br, I) but definitely excludes AlF_3 as a possible product of the reaction.

$AlF_2(OH)$ with a polymeric solid state structure of the known pyrochlore type represents the end product of the hydrolysis of $[Al(Py)_4F_2]Cl$ (**2a**). If the hydrolysis reaction was performed with very diluted solutions of hydrochloric acid in methanol, $[Al(H_2O)_4F_2]Cl{\cdot}2[PyH]Cl$ (**4**) was isolated as a new intermediate product besides the previously reported $[Al(Py)_4F_2]Cl{\cdot}2[PyH]Cl$.[7]

dx.doi.org/10.1021/ic301502u | Inorg. Chem. 2012, 51, 11612−11622

The presence of pyridinium chloride not only is necessary to avoid the condensation of $[Al(H_2O)_4F_2]Cl$ by HCl elimination, thus preventing formation of polymeric $AlF_2(OH)$ during or after the exchange of the pyridine ligands by water, but obviously plays an important role in the crystallization process of salts with $[Al(D)_4F_2]^+$ cations (D = pyridine or water).

$[Al(Py)_4F_2]Cl$ (**2a**) reacts with *cyclo-n*-propyl-phosphonic acid anhydride $[CH_3CH_2CH_2-PO_2]_3$ in pyridine at room temperature under cleavage of both Al−F bonds. The formed product possesses Al-atoms which are octahedrally coordinated by all 6 oxygen in the first and all 3 phosphorus in the second coordination spheres. Both fluorine atoms are bonded directly to phosphorus. The characterization of this amorphous compound giving unimpeachable proof for the unexpected F-migration from Al- to P-atoms in the course of the reaction clearly demonstrates the capacity of multinuclear solid state NMR spectroscopy as a reliable experimental basis in the studies of noncrystalline materials.

■ ASSOCIATED CONTENT

Supporting Information

CIF file. This material is available free of charge via the Internet at http://pubs.acs.org.

■ AUTHOR INFORMATION

Corresponding Author

*E-mail: erhard.kemnitz@chemie.hu-berlin.de.

Notes

The authors declare no competing financial interest.

■ ACKNOWLEDGMENTS

We thank Dr. Beatrice Braun and Dr. Stephan Mebs for crystallographic support, Dr. M. Feist for TG and DTA measurements, Prof. Christian Jaeger (BAM) for performing the 600 MHz Solid State NMR measurements and Dr. Gudrun Scholz for fruitful discussions. Funding from DAAD Bonn for a 3 month research fellowship (Kh.I.Kh) is gratefully acknowledged.

■ REFERENCES

(1) (a) Krespan, G. C.; Dixon, D. A. *J. Fluorine Chem.* **1996**, *77*, 117−126. (b) Krespan, G. C.; Petrov, V. A. *Chem. Rev.* **1996**, *96*, 3269−3301. (c) Petrov, V. A.; Krespan, G. C.; Smart, B. E. *J. Fluorine Chem* **1996**, *77*, 139−142. (d) Petrov, V. A.; Krespan, G. C.; Smart, B. E. *J. Fluorine Chem.* **1998**, *89*, 125−130. (e) Petrov, V. A.; Krespan, G. C. *J. Fluorine Chem.* **2000**, *102*, 199−204.

(2) Krahl, Th.; Stösser, R.; Kemnitz, E.; Scholz, G.; Feist, M.; Silly, G.; Buzaré, J.-Y. *Inorg. Chem.* **2003**, *42*, 6474−6483.

(3) Krahl, Th.; Kemnitz, E. *J. Fluorine Chem.* **2006**, *127*, 663−678.

(4) Krahl, Th.; Kemnitz, E. *Angew. Chem., Int. Ed.* **2004**, *43*, 6553−6556.

(5) Winfield, J. M. *J. Fluorine Chem.* **2009**, *130*, 1069−1079.

(6) Krahl, Th., PhD Thesis, Humboldt-Universität zu Berlin, 2005.

(7) Dimitrov, A.; Heidemann, D.; Kemnitz, E. *Inorg. Chem.* **2006**, *45*, 4952−4960.

(8) Kolf, S.; Preetz, W. *Z. Anorg. Allg. Chem.* **1997**, *623*, 501−508.

(9) Holzbock, J.; Sawodny, W.; Walz, L. *Z. Kristallogr.* **1997**, *212*, 115−120.

(10) Holzbock, J.; Sawodny, W.; Thewalt, U. *Z. Anorg. Allg. Chem.* **2000**, *626*, 2563−2568.

(11) Fochi, G.; Strähle, J.; Gingl, F. *Inorg. Chem.* **1991**, *30*, 4669−4671.

(12) Sheldrick, G. M. *Acta Crystallogr.* **1990**, *A46*, 467−473.

(13) Sheldrick, G. M. *SHELXL-97, Program for Crystal Structure Refinement*; University of Göttingen: Göttingen, 1997.

(14) Cory, D. G.; Ritchey, W. M. *J. Magn. Res.* **1988**, *80*, 128−132.

(15) Massiot, D.; Fayon, F.; Capron, M.; King, I.; Le Calvé, S.; Alonso, B.; Durand, J. O.; Bujoli, B.; Gan, Z.; Hoatson, G. *Magn. Reson. Chem.* **2002**, *40*, 70−76.

(16) JCPDS-ICCD-International Centre for Diffraction Data. PDF-2 Database, USA, Release 2001.

(17) Wilson, J. W.; Worrall, I. J. *J. Inorg. Nucl. Chem.* **1969**, *31*, 1205−1206.

(18) Wilson, J. W.; Worrall, I. J. *Inorg. Nucl. Chem. Lett.* **1967**, *3*, 57−60.

(19) Wilson, J. W.; Worrall, I. J. *J. Chem. Soc. A* **1968**, 316−317.

(20) Pullmann, P.; Hensen, K.; Bats, J. *Z. Naturforsch.* **1984**, *37b*, 1312−1315.

(21) Corey, J. Y.; Lamberg, R. *Inorg. Nucl. Chem. Lett.* **1972**, *8*, 275−280.

(22) Gorenbein, E.Ya.; Rucin, G. G.; Skorobogátko, E. P. *Žhurn. Neorg. Khim.* **1969**, 516−520.

(23) Troyanov, S. I. *Žhurn. Neorg. Khim.* **1994**, *39*, 552−555.

(24) Berg, R. W.; Poulsen, F. W.; Nielsen, K. *Acta Chem. Scand.* **1997**, *51*, 442−448.

(25) Troyanov, S. I.; Krahl, Th.; Kemnitz, E. *Z. Kristallogr.* **2004**, *219*, 88−92.

(26) Haraguchi, H.; Fujiwara, S. *J. Phys. Chem.* **1969**, *78*, 3467−3473.

(27) Kidd, R. G.; Truax, D. R *J. Am. Chem. Soc.* **1968**, *20*, 6867−6869.

(28) Cerny, Z.; Machcek, J.; Fusek, J.; Hermanek, S.; Kriz, O.; Casensky, B. *J. Organomet. Chem.* **1991**, *402*, 139−144.

(29) Akitt, J. W. *Prog. Nucl. Magn. Reson. Spectrosc.* **1989**, *21*, 1−149.

(30) Freude, D. Quadrupolar nuclei in solid-state nuclear magnetic resonance. In *Encyclopedia of Analytical Chemistry*; Meyers, R. A., Ed.; John Wiley & Sons Ltd: Chichester, 2000; pp 12188−12224.

(31) Müller, D.; Jahn, E.; Ladwig, G.; Haubenreisser, U. *Chem. Phys. Lett.* **1984**, *109*, 332−336.

(32) Lippmaa, E.; Samoson, A.; Mägi, M. *J. Am. Chem. Soc.* **1986**, *108*, 1730−1735.

(33) Müller, D.; Bentrup, U. *Z. Anorg. Allg. Chem.* **1989**, *575*, 17−25.

(34) Groß, U.; Müller, D.; Kemnitz, E. *Angew. Chem., Int. Ed.* **2003**, *42*, 2626−2629.

(35) König, R.; Scholz, G.; Scheurell, K.; Heidemann, D.; Buchem, I.; Unger, W.; Kemnitz, E. *J. Fluorine Chem.* **2009**, *131*, 91−97.

(36) Kemnitz, E.; Groß, U.; Rüdiger, S.; Scholz, G.; Heidemann, D.; Troyanov, S. I.; Morosov, I. V.; Lemée-Cailleau, M.-H. *Solid State Sci.* **2006**, *8*, 1443−1452.

(37) König, R; Scholz, G.; Pawlik, A.; Jäger, C.; van Rossum, B.; Oschkinat, H.; Kemnitz, E. *J. Phys. Chem. C* **2008**, *112*, 15708−15720.

(38) König, R; Scholz, G.; Pawlik, A.; Jäger, C.; van Rossum, B.; Kemnitz, E. *J. Phys. Chem. C* **2009**, *113*, 15576−15585.

(39) Han, O. H.; Oldfield, E. *Inorg. Chem.* **1990**, *29*, 3666−3669.

(40) Chu, P.-C.; de Mallmann, A.; Lunsford, J. H. *J. Phys. Chem.* **1991**, *95*, 7362−7368.

(41) Schurk o, R. W.; Wasylishen, R. E.; Phillips, A. D. *J. Magn. Reson.* **1998**, *133*, 388−394.

(42) Brandenburg, K.; Berndt, M. *Diamond 2.1c*; Crystal Impact GbR: Bonn, Germany, 1999.

(43) Jakobsmeier, L.; Krossing, I.; Nölth, H.; Schmidt, M. J. H. *Z. Naturforsch.* **1996**, *51b*, 1117−1126.

(44) Junk, P. C.; Scelton, B. W.; White, A. H. *Acta Crystallogr.* **2003**, *C 59*, m289−m290.

(45) Knabel, K.; Nölth, H. *Z. Naturforsch.* **2005**, *60b*, 1027−1035.

(46) Kiriazis, L.; Mattes, R. *Z. Anorg. Allg. Chem.* **1991**, *593*, 90−98.

(47) Zhang, L.; Eckert, H. *Solid State Nucl. Magn. Reson.* **2004**, *26*, 132−146.

(48) Egan, J. M.; Wenslow, R. M.; Mueller, K. T. *J. Noncryst. Solid* **2000**, *261*, 115−126.

(49) Lang, D. P.; Alam, T. M.; Bencoe, D. N. *Chem. Mater.* **2001**, *13*, 420−428.

(50) Chan, J. C. C.; Eckert, H. *J. Magn. Reson.* **2000**, *147*, 170−178.